Chinese Chemical Letters 37 (2026) 112813

Contents lists available at ScienceDirect

Chinese Chemical Letters

journal homepage: www.elsevier.com/locate/cclet

Structural and catalytic mechanisms of two *N*-hydroxycinnamoyltransferases underlying lycibarbarspermidines biosynthesis in wolfberry

Shao-Yang Li[1], Jia-Cheng Huang[1], Ya-Lin Wang, Hong-Ting Zhen, Yu Fan, Zheng-Qun Zhou, Guo-Dong Chen, Jian-Ming Lv, Gao-Qian Wang*, Dan Hu*, Hao Gao*

Institute of Traditional Chinese Medicine & Natural Products, College of Pharmacy/State Key Laboratory of Bioactive Molecules and Druggability Assessment/International Cooperative Laboratory of Traditional Chinese Medicine Modernization and Innovative Drug Development of Ministry of Education (MOE) of China/Guangdong Province Key Laboratory of Pharmacodynamic Constituents of TCM and New Drugs Research, Jinan University, Guangzhou 510632, China

ARTICLE INFO

Article history:
Received 21 January 2026
Revised 18 April 2026
Accepted 20 April 2026
Available online 22 April 2026

Keywords:
Wolfberry
Lycibarbarspermidines
Biosynthesis
N-Hydroxycinnamoyltransferases
Crystal structure
Catalytic mechanism

ABSTRACT

Lycibarbarspermidines represent a major class of bioactive components in wolfberry (the fruit of *Lycium barbarum*), consisting of di-phenylpropionyl spermidines and their glucosides. While the molecular basis underlying their glycodiversity was clarified in our previous work, the biosynthesis of di-phenylpropionyl spermidine core structure remains elusive. In particular, the acyltransferase responsible for conjugating dihydrocaffeoyl, one of the dominant phenylpropionyl moieties, is still unidentified. Herein, two *N*-hydroxycinnamoyltransferases (LbSCT1/2) from wolfberry were identified, which not only catalyze the conjugation of spermidine with caffeoyl-CoA, but also exhibit high catalytic activity toward dihydrocaffeoyl-CoA. Notably, LbSCT2 catalyzes monoacylation, whereas LbSCT1 enables sequential diacylation. Together with caffeoyl-CoA double bond reductase (LbDBR2), LbSCT1/2 accomplish the biosynthesis of lycibarbarspermidine I-IV. Furthermore, LbSCT1 efficiently catalyzes the biosynthesis of kukoamine B, a major bioactive component from *Lycii Cortex* (the root bark of *Lycium* species). Crystal structural and mutagenic investigations elucidated the catalytic mechanisms underlying the selectivity of LbSCT1/2 for spermidine mono- and diacylation. This study establishes the complete biosynthesis of lycibarbarspermidines and provides valuable enzymatic tools for diversifying phenylpropionyl compounds.

© 2026 Published by Elsevier B.V. on behalf of Chinese Chemical Society and Institute of Materia Medica, Chinese Academy of Medical Sciences.

Wolfberry, the fruit of *Lycium barbarum*, is a classic traditional Chinese medicine (TCM) with a long history of dual food-medicine applications, and ranks among China's major exported medicinal materials and decoction pieces [1]. Its constituents include polysaccharides, carotenoids, general phenolic components, phenylpropionyl aromatic amines, and phenylpropionyl aliphatic amines [2]. Among these, phenylpropionyl aliphatic amines represent a major class of bioactive constituents of wolfberry identified in recent years [3–5]. They are characterized by an aliphatic amine core, with spermidine serving as the primary backbone, alongside minor structural analogues such as spermine, putrescine, and agmatine. This aliphatic amine skeleton is conjugated with one or two phenylpropionyl moieties. Particularly, the di-phenylpropionyl spermidines, termed lycibarbarspermidines, account for over 1 % of the fruit content and represent the predominant form of phenylpropionyl aliphatic amines [4–6]. The structural diversity of lycibarbarspermidines is initially driven by the conjugation of spermidine at the N1 and N10 positions with identical or distinct phenylpropionyl units, with further structural diversification achieved by glycosylation. These lycibarbarspermidines exhibit remarkable biological activities in the nervous and metabolic systems, which are consistent with the traditional therapeutic effects of wolfberry, and have been identified as geographical characteristics of wolfberry from Ningxia, China [4–9].

While the catalytic mechanism governing the glycodiversity of lycibarbarspermidines has been previously elucidated by our research group [10], the enzymatic basis responsible for assembling the di-phenylpropionyl spermidine core structure remains elusive. The phenylpropionyl moieties of the core structure are dominated by caffeoyl and dihydrocaffeoyl groups, accompanied by minor analogs including *cis*-caffeoyl, feruloyl,

* Corresponding authors.
E-mail addresses: tghao@jnu.edu.cn (H. Gao), thudan@jnu.edu.cn (D. Hu), gqwang@jnu.edu.cn (G.-Q. Wang).
[1] These authors contributed equally to this work.

https://doi.org/10.1016/j.cclet.2026.112813
1001-8417/© 2026 Published by Elsevier B.V. on behalf of Chinese Chemical Society and Institute of Materia Medica, Chinese Academy of Medical Sciences.

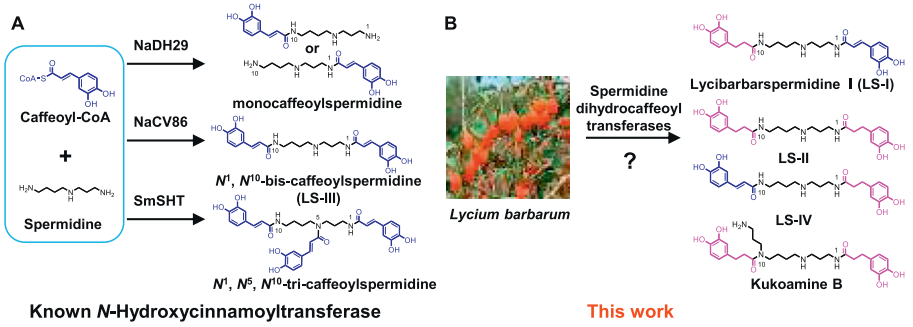


Fig. 1. Representative *N*-hydroxycinnamoyltransferases. (A) Plant-derived *N*-hydroxycinnamoyltransferases catalyzing mono-, di-, and triacylation. (B) Chemical structures of lycibarbarspermidine I, II, IV and kukoamine B bearing dihydrocaffeoyl groups from *Lycium barbarum*.

p-coumaroyl moieties. Notably, the dihydrocaffeoyl moiety is present in three of the four representative di-phenylpropionyl spermidine core structures (lycibarbarspermidines I-IV), and the acyltransferase responsible for dihydrocaffeoyl conjugation has not yet been identified. In detail, lycibarbarspermidine I (LS-I) is N^1-caffeoyl-N^{10}-dihydrocaffeoylspermidine, LS-II is N^1,N^{10}-bis-dihydrocaffeoylspermidine, LS-III is N^1,N^{10}-bis-caffeoylspermidine and LS-IV is N^1-dihydrocaffeoyl-N^{10}-caffeoylspermidine (Fig. 1). These representative core structures provide an ideal opportunity to dissect the asymmetric conjugation of spermidine with caffeoyl and dihydrocaffeoyl moieties, thereby fully elucidating the complete biosynthetic pathway of lycibarbarspermidines. Furthermore, kukoamine B, the pharmacologically active constituent of *Lycii Cortex* (the root bark of *Lycium* species) [11], is a representative dihydrocaffeoyl spermine derivative that exhibits high structural similarity to LS-II and may therefore possess a similar yet uncharacterized biosynthetic pathway.

Phenylpropionyl aliphatic amines are generated by *N*-hydroxycinnamoyltransferases, which catalyze the amide conjugation of phenylpropionyl moieties to aliphatic polyamines [12]. These key enzymes belong to the BAHD acyltransferase family and are ubiquitously distributed across the plant kingdom [13]. Currently identified *N*-hydroxycinnamoyltransferases can mediate the ligation of acyl donors including *p*-coumaroyl-CoA, caffeoyl-CoA and feruloyl-CoA to polyamines [14]. To date, multiple spermidine caffeoyltransferases (SCT) have been identified. For instance, NaDH29 and NaCV86 from *Nicotiana attenuate* mediate mono- and dicaffeoylation of spermidine, respectively, while SmSHT from *Solanum melongena* is involved in tricaffeoylspermidine biosynthesis (Fig. 1A) [15–17]. However, enzymes that utilize saturated dihydrocaffeoyl-CoA as an acyl donor have yet to be discovered. In particular, wolfberry accumulates unique metabolites including LS-I and LS-IV, which harbor two caffeoyl moieties with different saturation levels at the N1 and N10 positions of spermidine (Fig. 1B). This leaves an unresolved question as to whether their biosynthesis is catalyzed by a specific single acyltransferase or stepwise by distinct acyltransferases as observed for NaDH29 and NaCV86 [18]. Furthermore, the molecular mechanisms underlying the selective catalysis of spermidine mono- or diacylation remain poorly understood.

To elucidate the biosynthesis of di-phenylpropionyl spermidines, the full-length transcriptome sequencing of *L. barbarum* was performed [10]. We first searched for double-bond reductases (DBR) in wolfberry using MdHCDBR and NtDBR as queries. MdHCDBR is a nicotinamide adenine dinucleotide phosphate (NADPH)-dependent double-bond reductase from *Malus domestica* Borkh. (apple) that converts *p*-coumaroyl-CoA to dihydrocoumaroyl-CoA, whereas NtDBR is a medium-chain dihydroreductase derived from *Nicotiana tabacum* that exhibits broad substrate promiscuity and catalyzes the double bond reduction of

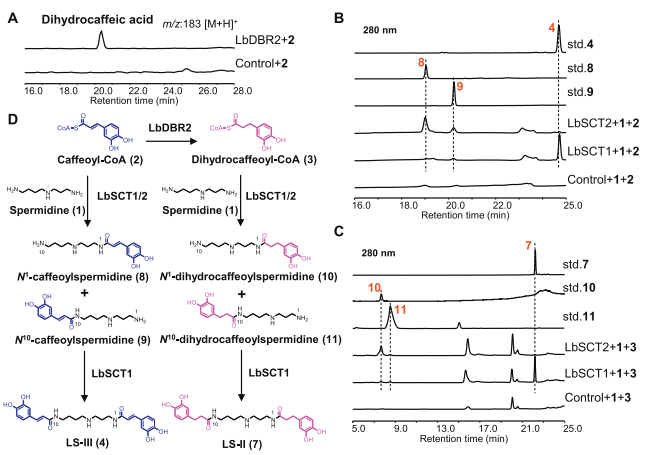


Fig. 2. Identification of LbDBR2 and LbSCT1/2 involved in lycibarbarspermidines biosynthesis. (A) Extracted ion chromatograms (EIC) profiles of *in vitro* assays of LbDBR2 with substrate **2**. (B, C) HPLC profiles of reactions of LbSCT1/2, using acyl donors **2** or **3** in separate reactions with substrate **1**. (D) Reaction schemes for the formation of LS-II and LS-III catalyzed by LbDBR2 and LbSCT1/2.

cinnamaldehyde-like substrates [19,20]. Three putative reductases, LbDBR1–3, were identified from *L. barbarum* and share >70 % homology with the above two enzymes (Fig. S1 in Supporting information).

For functional characterization of LbDBR1–3, the proteins were expressed by *Escherichia coli* BL21 (DE3) and purified by Ni-NTA chromatography [21,22]. The caffeoyl-CoA (**2**) was first used as a substrate to conduct the enzymatic reaction. To facilitate the visualization of the intended product dihydrocaffeoyl-CoA (**3**) by liquid chromatography-mass spectrometry (LC-MS), we performed the base-catalyzed hydrolysis of the reaction products. As a result, dihydrocaffeic acid was only detected in the catalyzed reaction of LbDBR2 (GenBank accession number: XM_060317769) (Fig. 2A and Fig. S2 in Supporting information). To rule out the possibility that dihydrocaffeic acid was directly generated from caffeic acid, caffeic acid was incubated with LbDBR2 and no conversion was observed (Fig. S3 in Supporting information). Moreover, none of the three enzymes could catalyze the reduction of LS-III (**4**) to **5** or **7** (Fig. S4 in Supporting information). In addition, LbDBR2 is capable of catalyzing the double bond reduction of both *p*-coumaroyl–CoA and feruloyl–CoA, indicative of its broad substrate tolerance (Fig. S5 in Supporting information). These results suggest that the biosynthesis of lycibarbarspermidines containing dihydrocaffeoyl moiety might be initiated by the formation of **3** *via* LbDBR2, which is then transferred to N1/N10 of the spermidine by novel *N*-hydroxycinnamoyltransferase-like enzymes (Fig. 2D).

To address this hypothesis, ten candidate genes with homology to known *N*-hydroxycinnamoyltransferases were screened from *L. barbarum*. Phylogenetic analysis of these candidate genes alongside characterized enzymes led to the selection of LbSCT1/2 for further investigation, as they cluster with NaDH29 and NaCV86, which catalyze the two successive *N*-acylation reactions of spermidine in a stepwise manner (Fig. S6 in Supporting information) [15,18]. To elucidate the functions of LbSCT1/2 (GenBank accession numbers: XM_060333417; XM_060353499), the recombinant LbSCT1/2 proteins were obtained and incubated with spermidine (**1**) and acyl donors (Fig. S7 in Supporting information). As shown in Fig. 2B, LbSCT1 catalyzed spermidine (**1**) and caffeoyl-CoA (**2**) to generate diacylated product **4** as the major product, along with trace amounts of monocaffeoylspermidines **8** and **9**. In contrast, LbSCT2 predominantly produced **8**, minor amounts of **9**, and only trace levels of product **4** (Fig. 2B). All these products were unambiguously identified by comparison with authentic standards (Fig. S8 in Supporting information). To further verify the catalytic activity of LbSCT1/2 toward dihydrocaffeoyl-CoA (**3**), we performed enzymatic assays using **1** and **3** as substrates. The results revealed that LbSCT1 converted the substrates to yield LS-II (**7**) as the major product and trace amounts of monoacylated products **10** and **11** (Fig. 2C). By comparison, LbSCT2 mainly generated *N*1-acylated spermidine **10** with a small quantity of **11**, and yielded negligible amounts of the diacylated product (Fig. 2C). Collectively, these experiments demonstrated that both LbSCT1 and LbSCT2 possess the capacity to catalyze caffeoyl-CoA and dihydrocaffeoyl-CoA simultaneously. LbSCT1 primarily mediates the biosynthesis of diacylated spermidine, whereas LbSCT2 predominantly catalyzes the production of monoacylated spermidines with a strong regioselective preference for acylation at the N1 position (Fig. 2D).

To determine the sequential order of LbSCT1-catalyzed double acylation of spermidine, we performed enzymatic reactions using each of the four monoacylated spermidines **8**–**11** as acceptor substrates, with caffeoyl-CoA (**2**) and dihydrocaffeoyl-CoA (**3**) as acyl donors, respectively. The results showed that LbSCT1 catalyzed the acylation of two monoacylated spermidines (**8** and **9**) with caffeoyl-CoA to generate LS-III (**4**) (Figs. 3A and E). In addition, LbSCT1 catalyzed the reactions of compounds **8** and **9** with dihydrocaffeoyl-CoA (**3**), generating LS-I (**5**) and LS-IV (**6**), respectively (Figs. 3B and F, Fig. S8 in Supporting information). When mono-dihydrocaffeoylspermidines **10** and **11** were used as substrates, LbSCT1 catalyzed the conjugation of caffeoyl-CoA to both compounds, producing the corresponding products **6** and **5** (Figs. 3C and G); it also catalyzed the ligation of dihydrocaffeoyl-CoA to **10** or **11** to form LS-II (**7**) (Figs. 3D and H). Taken together, these results demonstrate that LbSCT1 can utilize four different monoacylated spermidines as acyl acceptors without preference, reacting with caffeoyl-CoA or dihydrocaffeoyl-CoA to generate lycibarbarspermidine I-IV.

Based on the results above, we hypothesized that di-phenylpropionyl spermidines might be biosynthesized *via* the synergistic catalysis of spermidine by LbSCT1 and LbSCT2. To validate this hypothesis, we co-incubated the two enzymes with spermidine (**1**), caffeoyl-CoA (**2**), and dihydrocaffeoyl-CoA (**3**) in a single reaction system. Subsequent comparison with authentic standards confirmed the successful production of four di-phenylpropionyl spermidines (**4**–**7**), with compound **7** being the most abundant (Figs. 4A and B). Herein, for the first time, we have elucidated the complete biosynthetic pathway of di-phenylpropionyl spermidines lycibarbarspermidine I-IV: firstly, LbDBR2 catalyzes the reduction of caffeoyl-CoA to generate dihydrocaffeoyl-CoA; subsequently, the *N*-hydroxycinnamoyltransferase LbSCT2 mediates the conjugation of caffeoyl-CoA or dihydrocaffeoyl-CoA to spermidine, yielding monoacylated spermidines; finally, LbSCT1 catalyzes the second-step acylation with (dihydro)caffeoyl-CoA to form di-

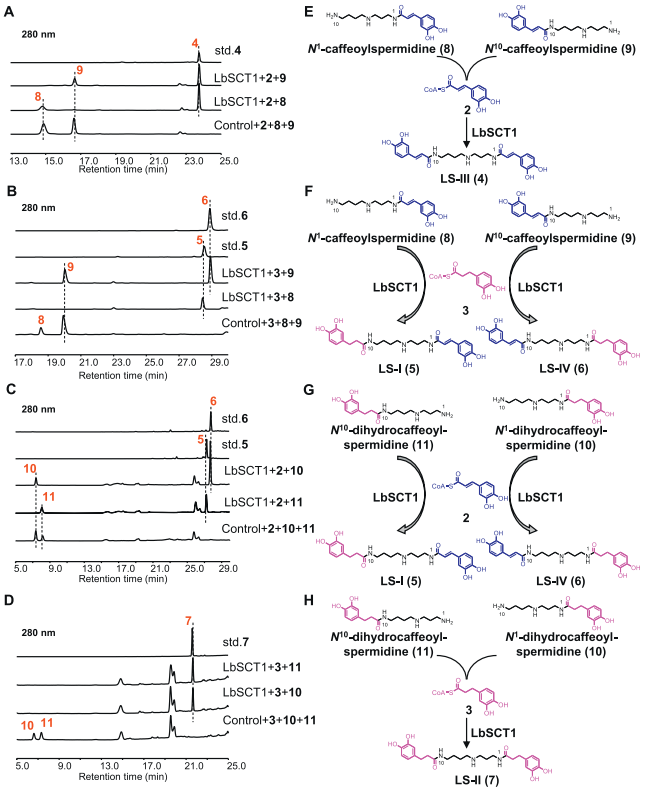


Fig. 3. Characterization of LbSCT1's second-step acylation capacity in lycibarbarspermidine I-IV biosynthesis. (A-D) HPLC profiles of LbSCT1 reactions using **8**–**11** as acyl acceptors to react with **2** or **3** separately. (E-H) The second-step acylation reactions of LbSCT1 during the biosynthesis of lycibarbarspermidine I-IV.

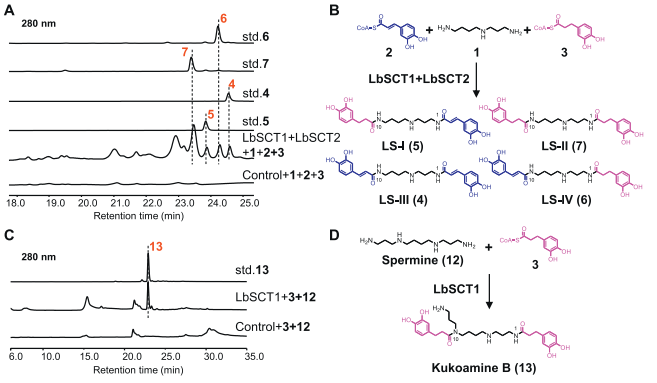


Fig. 4. Combined catalysis of LbSCT1/2 for lycibarbarspermidine I-IV and biosynthesis of kukoamine B catalyzed by LbSCT1. (A, B) HPLC profiles and reaction schemes for the biosynthesis of lycibarbarspermidine I-IV mediated by the combined catalysis of LbSCT1/2 with substrates **1**, **2**, and **3**. (C, D) HPLC profiles and reaction schemes for the formation of kukoamine B catalyzed by LbSCT1 with substrates **3** and **12**.

phenylpropionyl spermidines. Notably, LbSCT1 alone can catalyze the double acylation of spermidine to directly generate products **4** and **7**.

Collectively, these results clearly demonstrate that LbSCT1 and LbSCT2 can catalyze the acylation of spermidine with both caffeoyl-CoA and dihydrocaffeoyl-CoA, with LbSCT2 specialized in monoacylation and LbSCT1 capable of sequential diacylation. To further characterize the catalytic properties of LbSCT1/2, caffeoyl-CoA was used as the acyl donor substrate for subsequent assays. The recombinant LbSCT1/2 proteins exhibited maximal catalytic

activity at 37 °C; LbSCT1 displayed the highest catalytic efficiency at pH 8.0, while LbSCT2 achieved optimal catalytic activity at pH 8.5 (Fig. S9 in Supporting information). Kinetic parameters of LbSCT1/2 for caffeoyl-CoA and dihydrocaffeoyl-CoA were calculated based on the Michaelis-Menten equation, with the K_m, k_{cat}, and k_{cat}/K_m N values summarized in the Supplementary Table S3 (Fig. S10 in Supporting information). These results revealed that both LbSCT1 and LbSCT2 exhibited higher catalytic efficiency toward dihydrocaffeoyl-CoA.

Since LbSCT1 catalyzes dihydrocaffeoylation at the N1 and N10 positions of spermidine with dihydrocaffeoyl-CoA, these acylation sites are identical to those of dihydrocaffeoylation in kukoamine B (**13**), a characteristic constituent of *Lycium* species and predominantly accumulates in the root bark of *Lycium barbarum* and *Lycium chinense* [11]. Thus, we hypothesized that LbSCT1 might be responsible for catalyzing the dihydrocaffeoylation of spermine to biosynthesize kukoamine B. To validate this hypothesis, we performed the enzymatic reaction under identical conditions using spermine (**12**) as the alternative substrate with dihydrocaffeoyl-CoA (**3**). The formation of kukoamine B was unambiguously confirmed by comparison with an authentic standard (Figs. 4C and D, Fig. S8 in Supporting information). Furthermore, to investigate the substrate promiscuity of LbSCT1 and LbSCT2 toward phenylpropanoyl donors, we performed enzymatic reactions using *p*-coumaroyl-CoA and feruloyl-CoA. LC-MS analysis revealed that both enzymes could catalyze the conjugation of these two acyl donors with spermidine to yield the corresponding products (Fig. S11 in Supporting information). Consistent with previous results, LbSCT1 primarily catalyzed diacylation, whereas LbSCT2 predominantly generated monoacylated products. These results demonstrate that both LbSCT1 and LbSCT2 exhibit substrate promiscuity, highlighting their potential as biocatalysts for phenylpropanoylation.

To elucidate the structural basis for the catalytic selectivity of LbSCT1/2, we attempted to obtain co-crystal structures of LbSCT1/2 in complex with spermidine and various acyl donors. Following a series of co-crystallization and soaking experiments, we successfully determined the complex crystal structure of LbSCT1-spermidine at a resolution of 2.12 Å (PDB ID: 22IT). LbSCT1 represents the first *N*-hydroxycinnamoyltransferase catalyzing dihydrocaffeoyl-CoA with a solved protein crystal structure, which is similar to known BAHD family acyltransferases, exhibiting a compact α/β architecture. Its N-terminal domain (residues 1–184 and 381–404) harbors the conserved BAHD acyltransferase motifs "HXXXD" and "DFGWG", linked to the C-terminal domain (residues 229–380, 405–452) *via* a flexible bridging loop (residues 185–228) (Fig. 5A) [23]. A solvent channel between domains allows bilateral access of acyl donors/acceptors for catalysis in the active pocket [24]. Two well-defined spermidine electron density maps were detected in its structure: one at the acyl acceptor site near catalytic residue His164, and the other at the acyl donor pocket, likely owing to spermidine being a flexible linear small molecule that readily diffuses into the protein cavity (Fig. S12 in Supporting information). Structural alignment *via* the Dali server with other *N*-hydroxycinnamoyltransferases revealed that LbSCT1 shares high structural similarity with feruloyl-CoA monoacyltransferase AsFMT from *Angelica sinensis* (PDB ID: 7W26) and *Rauvolfia serpentina* vinorine synthase *VS* (PDB ID: 2BGH), with root mean square deviation (RMSD) values of 2.362 Å (over 371 Cα atoms) and 2.832 Å (over 257 Cα atoms), respectively (Fig. S13 in Supporting information) [25,26]. Although LbSCT2 protein crystals were unavailable, we predicted its structure *via* AlphaFold2 (Fig. 5B) [27,28]. Given the 51 % amino acid sequence identity between LbSCT1 and LbSCT2, their RMSD across 373 Cα atoms was 1.066 Å. All these enzymes contain the conserved BAHD motifs, with the catalytic His residue that initiates the acylation reaction exposed within the solvent channel (Fig. S13 in Supporting information). These structural insights enable the analysis of enzyme catalytic pockets to facilitate further mechanistic investigations.

Although both LbSCT1 and LbSCT2 can catalyze the formation of amide bonds between caffeoyl-CoA/dihydrocaffeoyl-CoA and spermidines, LbSCT2 only mediates the monoacylation of spermidine, whereas LbSCT1 can catalyze the sequential conjugation of two molecules of acyl donor to the acceptor. In order to investigate the catalytic mechanisms underlying the mono-/diacylation of substrates catalyzed by LbSCT1/2, we compared the protein structures of LbSCT1 and LbSCT2, and analyzed the amino acid residues within a radius of 5 Å around the two spermidines in the catalytic pockets. In the LbSCT1 structural model, H164, D168 and W414 within the conserved motifs of the BAHD family are positioned around spermidine and function as conserved catalytic residues, confirmed by drastically reduced activity upon their mutation to alanine (A) (Figs. 5C and D). Furthermore, comparative analysis of their catalytic pockets revealed that most amino acid residues within 5 Å of spermidine are identical or highly similar. We therefore performed site-directed mutagenesis assays targeting residues with significant differences, substituting I162, T172, M173 and A312 of LbSCT1 with the corresponding amino acids from LbSCT2. Enzymatic assays using optimal substrate dihydrocaffeoyl-CoA as an acyl donor showed that the I162C, T172A and M173F mutants exhibit a significant reduction in catalytic activity (Figs. 5C and D). These results indicate that these three residues likely maintain the stable conformation of the substrate within the solvent channel *via* hydrophobic interactions, thereby playing critical roles in the catalytic process of LbSCT1.

Notably, the A312I mutant of LbSCT1 exhibited diminished catalytic activity, yet the proportion of N^{10}-dihydrocaffeoylspermidine (**11**) was significantly increased (Fig. 5D). The same phenomenon was observed when caffeoyl-CoA (**2**) was employed as the acyl donor (Fig. S14 in Supporting information). To clarify the factors leading to the changes in product distribution, we performed enzymatic reactions using monoacylated spermidines (**8**–**11**) with caffeoyl-CoA and dihydrocaffeoyl-CoA. The results showed that the A312I mutant exhibited significant inhibition on the conversion rate of N^{10}- (dihydro)caffeoylspermidine (Table S5 in Supporting information), indicating that A312I mutant selectively influences the second-step acylation of mono-(dihydro)caffeoylspermidine at the N1 position, which might be attributed to the increased steric hindrance and hydrophobicity within the solvent channel resulting from the introduction of isoleucine (I). The mutation of A312 to phenylalanine (F), which possesses a bulkier side chain, resulted in a significant reduction in overall catalytic activity, further supporting the hypothesis (Fig. 5D). Collectively, the A312 residue may modulate the mono-/diacylation function of LbSCT1 toward spermidine *via* a steric hindrance effect.

In addition to the active site, we observed significant structural differences in the acyl acceptor entry channels of LbSCT1 and LbSCT2. LbSCT1 features a wider solvent channel, whereas LbSCT2 contains a lysine residue (K217) at the entry site that narrows the channel (Fig. 5E), which may contribute to the limited capacity of LbSCT2 to produce diacylated spermidine. To test this hypothesis, we constructed the K217G mutant of LbSCT2. Enzymatic activity assays demonstrated a significant increase in the yield of dicaffeoylspermidine (Fig. 5E and Fig. S15 in Supporting information). These data indicate that the dimensions of the acyl receptor channel entrance represent a critical role influencing the second-step acylation. Additionally, we analyzed the substrate entry channels of three representative *N*-hydroxycinnamoyltransferases: NaDH29 from *N. attenuata* for monoacylation (with a structure predicted by AlphaFold2), AtSDT (PDB: 6LPW) and AtSHT (PDB: 6LPV) from *Arabidopsis thaliana*, which function as di- and tri-acylation specific enzymes, respectively [15,23]. Compared with the broad acyl acceptor entry channels of AtSDT and AtSHT, the entry channel of

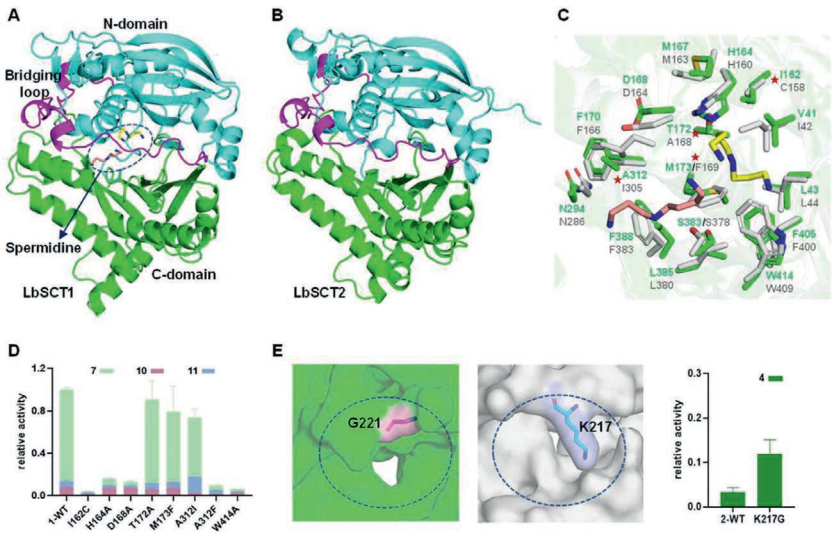


Fig. 5. Structural studies of LbSCT1 and LbSCT2. (A) Overall structure of LbSCT1 bound with spermidine, contains N-domain (colored in cyan), C-domain (colored in green) and a bridging loop (colored in magenta). Spermidines occupying the acyl donor and acceptor binding sites are shown as pink and yellow sticks, respectively. (B) Overall structure of LbSCT2 predicted by Alphafold2. (C) Superposition of LbSCT1 (green) and LbSCT2 (gray). Residues and spermidine are shown in sticks. The difference residues are marked with an asterisk. (D) The relative activities of LbSCT1 mutants at the active site. (E) The acyl-acceptor entrance of LbSCT1 and LbSCT2 and the relative activities of mutants at the entrance. Data represent mean ± SD ($n = 3$).

NaDH29 is also occluded by a lysine residue K226 (Fig. S16 in Supporting information). These findings suggest that the multisite acylation activity of plant-derived *N*-hydroxycinnamoyltransferases is modulated by their substrate entry channel characteristics.

In summary, we functionally characterized a caffeoyl-CoA double bond reductase (LbDBR2) and two *N*-hydroxycinnamoyltransferases (LbSCT1/2), which are responsible for the biosynthesis of lycibarbarspermidines, the major bioactive ingredients of wolfberry. Notably, LbSCT1 and LbSCT2 not only catalyze the conjugation of spermidine with caffeoyl-CoA but also exhibit stronger catalytic activity toward dihydrocaffeoyl-CoA. Specifically, LbSCT2 exerts monoacylation activity, whereas LbSCT1 uniquely catalyzes the sequential diacylation. Furthermore, LbSCT1 mediates spermine double dihydrocaffeoylation to generate kukoamine B, a major bioactive component from the *Lycii Cortex*. Crystal structure analysis and mutagenesis assays revealed that the residue A312 in the active site of LbSCT1, as well as the dimensions of the acyl receptor channel entry, critically affects the capacity for the second-step acylation. Our study elucidates the key enzymes catalyzing the formation of the core structure of representative di-phenylpropionyl spermidines, thereby completing the full elucidation of the biosynthetic pathway of lycibarbarspermidines, and enhances the understanding of the molecular mechanisms underlying the mono- and diacylation of *N*-hydroxycinnamoyltransferases.

CRediT authorship contribution statement

Shao-Yang Li: Writing – original draft, Validation, Investigation. **Jia-Cheng Huang:** Validation, Investigation. **Ya-Lin Wang:** Investigation. **Hong-Ting Zhen:** Validation, Investigation. **Yu Fan:** Investigation. **Zheng-Qun Zhou:** Investigation. **Guo-Dong Chen:** Investigation. **Jian-Ming Lv:** Investigation. **Gao-Qian Wang:** Writing – review & editing, Supervision, Conceptualization. **Dan Hu:** Writing – review & editing, Supervision, Conceptualization. **Hao Gao:** Writing – review & editing, Supervision, Conceptualization.

Declaration of competing interest

The authors declare that they have no known competing financial interests or personal relationships that could have appeared to influence the work reported in this paper.

Acknowledgments

This work was financially supported by grants from the Guangdong Major Project of Basic and Applied Basic Research (No. 2023B0303000026), the National Natural Science Foundation of China (Nos. 82321004, U24A20782, 82504640), the 111 Project of Ministry of Education of the People's Republic of China (No. B25061), Guangdong Special Support Program (Nos. 2025JC09Y089, 2024TX08A045), the Guangdong International Science and Technology Cooperation Base (No. 2021A0505020015), the Guangdong Basic and Applied Basic Research Foundation, China (Nos. 2026A1515010574, 2023B1515040016, 2023A1515110388), the Innovative and Research Teams Project of Guangdong Higher Education Institution (No. 2021KCXTD001), the Guangzhou Science and Technology Project, China (Nos. 202206010020, 2024A04J6241), the Fundamental Research Funds for the Central Universities (Nos. 21625208, 21625349), and the National Innovation and Entrepreneurship Training Program For Undergraduate (No. 202510559068). We thank the staff at beamline BL02U1 of the Shanghai Synchrotron Radiation Facility for assistance during data.

Supplementary materials

Supplementary material associated with this article can be found, in the online version, at doi:10.1016/j.cclet.2026.112813.

References

[1] Y. Fang, M.X. Tang, X. Liu, Front. Public Health 12 (2025) 1508839.
[2] D. Qian, Y.X. Zhao, G. Yang, et al., Molecules 22 (2017) 911.
[3] M. Ye, World J. Tradit. Chin. Med. 12 (2026) 129–133.
[4] W.Y. Sun, Z.H. Luo, J.Q. Cai, et al., Sci. Bull. 70 (2025) 3748–3752.
[5] Z.Q. Zhou, H.X. Fan, R.R. He, et al., J. Agric. Food Chem. 64 (2016) 2223–2237.
[6] Z.Q. Zhou, H.X. Fan, R.R. He, et al., World J. Tradit. Chin. Med. 2 (2016) 1–5.
[7] X.N. Zhang, X.Y. Wen, D. Zhou, et al., J. Ethnopharmacol 320 (2024) 117419.
[8] X.N. Zhang, X.Y. Wen, D. Zhou, et al., J. Agric. Food Chem. 73 (2025) 12723–12733.
[9] J.H. Guo, S.K. Gong, X.X. Zhang, et al., World J. Tradit. Chin. Med. 11 (2025) 77–102.
[10] S.Y. Li, G.Q. Wang, L. Long, et al., Nat. Commun. 15 (2024) 4588.
[11] Y.Y. Li, D.A. Stewart, X.M. Ye, et al., Front. Pharmacol. 9 (2019) 1575.
[12] D.M. Macoy, W.Y. Kim, S.Y. Lee, et al., Plant Biotechnol. Rep. 9 (2015) 269–278.
[13] J.C. D'Auria, Curr. Opin. Plant Biol. 9 (2006) 331–340.
[14] M. Roumani, S. Besseau, D. Gagneul, et al., J. Exp. Bot. 72 (2021) 2334–2355.

[15] N. Onkokesung, E. Gaquerel, H. Kotkar, et al., Plant Physiol. 158 (2012) 389–407.
[16] J.H. Liu, Y. Yuan, C. Wu, et al., PLoS One 8 (2013) e77275.
[17] H. Peng, T. Yang, B.D. Whitaker, et al., Hortic. Res. 3 (2016) 16062.
[18] H. Peng, R.S. Meyer, T. Yang, et al., BMC Plant Biol. 19 (2019) 261.
[19] M. Ibdah, A. Berim, S. Martens, et al., Phytochemistry 107 (2014) 24–31.
[20] D.J. Mansell, H.S. Toogood, J. Waller, et al., ACS Catal. 3 (2013) 370–379.
[21] X.C. Sun, Y.X. Wang, C.K. Li, et al., Chin. Chem. Lett. 36 (2025) 110895.
[22] K.Y. Wang, B.Y. Liu, D.J. Yan, et al., Chin. Chem. Lett. 36 (2025) 109811.
[23] C.Y. Wang, J.X. Li, M.L. Ma, et al., Front. Plant Sci. 11 (2021) 610118.
[24] W.T. Sun, L. Xiang, R.M. Wang, et al., Chin. Chem. Lett. 37 (2026) 110965.
[25] X. Liu, S.L. Dai, Y. Zhou, et al., Biochem. Biophys. Res. Commun. 594 (2022) 8–14.
[26] S.O. Shobade, M. Nilsen-Hamilton, O.A. Zabotina, Plants 14 (2025) 2069.
[27] J. Jumper, R. Evans, A. Pritzel, et al., Nature 596 (2021) 583–589.
[28] J.J. Zhou, Z.L. Wang, M. Zhang, et al., Chin. Chem. Lett. 36 (2025) 110805.